PERFORMANCE EVALUATION OF SYNTHETIC STORM TECHNIQUE OVER A TROPICAL REGION FOR RAIN ATTENUATION TIME SERIES GENERATION AT Ka-BAND

M.Sc. Thesis

By:
Maneesh Bazgalia

DEPARTMENT OF ASTRONOMY, ASTROPHYSICS AND SPACE ENGINEERING

INDIAN INSTITUTE OF TECHNOLOGY INDORE

June, 2021

PERFORMANCE EVALUATION OF SYNTHETIC STORM TECHNIQUE OVER A TROPICAL REGION FOR RAIN ATTENUATION TIME SERIES GENERATION AT Ka-BAND

A THESIS

Submitted in partial fulfillment of the requirements for the award of the degree
of
Master of Science

by
Maneesh Bazgalia

DEPARTMENT OF ASTRONOMY, ASTROPHYSICS AND SPACE ENGINEERING

INDIAN INSTITUTE OF TECHNOLOGY INDORE

June, 2021

INDIAN INSTITUTE OF TECHNOLOGY INDORE

CANDIDATE'S DECLARATION

I hereby certify that the work which is being presented in the thesis entitled **"Performance evaluation of synthetic storm technique over a tropical region for rain attenuation time series generation at Ka-band "** in the partial fulfillment of the requirements for the award of the degree of MASTER OF SCIENCE and submitted in the DEPARTMENT OF ASTRONOMY, ASTROPHYSICS AND SPACE ENGINEERING, Indian Institute of Technology Indore, is an authentic record of my own work carried out during the time period from July 2020 to May 2021 under the supervision of Dr. Saurabh Das. The matter presented in this thesis has not been submitted by me for the award of any other degree of this or any other institute.

10/6/2021
Maneesh Bazgalia
Signature with date
(Maneesh Bazgalia)

This is to certify that the above statement made by the candidate is correct to the best of my knowledge.

S. Das
10/6/2021
Signature of the Supervisor of
M.Sc. thesis (with date)
(Dr. Saurabh Das)

Maneesh Bazgalia has successfully given his M.Sc. Oral Examination held on **9th June 2021**

S. Das
Signature of M.Sc. thesis Supervisor
Date: 10/6/2021

Suman Majumdar 10/06/2021
Convener, DPGC
Date:-

Signature of M.Sc. coordinator
DAASE
Date:- 10-06-2021

Signature of Head of Department
DAASE
Date:- 10/06/2021

Saptarshi Ghosh
Signature of PSPC Member 1
Date:- 10/06/2021

10/06/2021
Signature of PSPC Member 2
Date:-

Acknowledgement

It has been an incredible journey for me while working on this project, **“Performance evaluation of synthetic storm technique over a tropical region for rain attenuation time series generation at Ka-band ”** for a few months. With the investment of time and effort, I learned something new and found some results. I want to express my most profound gratefulness to my supervisor **Dr. Saurabh Das**, for allowing me to work under him and provide excellent guidance, encouragement, moral support, and continuous assistance throughout this project. I would also like to thank my PSPC members **Dr. Saptarshi Ghosh** and **Dr. Siddharth Savyasachi Malu**, for their valuable scrutiny and feedback on my project at regular intervals. Last but not least, I would also like to thank my parents, family, colleagues for their motivation and constant support.

Abstract

Rainfall can result in the poor performance of satellite communication links primarily performing at frequencies larger than 10 GHz. Therefore, it is challenging to design Earth-satellite communication links in regions of heavy rainfall. Understanding the rain attenuation characteristics can help to improve the performance of satellite communication links. However, actual rain attenuation data may not be available, and hence an alternate way of obtaining rain attenuation characteristics is required. In the absence of actual data, estimated rain attenuation plays a vital role in analysing attenuation due to rain. ITU-R rain attenuation model is extensively used for statistical rain attenuation prediction. On the other hand, Synthetic storm technique (SST) is a conversion technique applied to obtain rain attenuation data using rain data. This work is focused on the effectiveness of the synthetic storm model for conversion of experimentally obtained data of rainfall rate into attenuation data due to rain. Matchings are observed between the measurements and estimation using the SST model.

Keywords: Synthetic storm technique (SST), rainfall rate, time series, rain attenuation

Contents

1 Introduction **1**

2 The Synthetic Storm Technique **4**

2.1 Fundamentals of the Synthetic Storm Technique 4

2.2 Two layer Precipitation model 5

2.3 SST Model 6

2.4 Variation of k and α with frequency (GHz) 9

3 Earlier work and other prediction models: **12**

4 Experimental Data **13**

5 Rain attenuation from measured data **14**

6 Rain Attenuation Dynamics **18**

6.1 The necessity for Fade slope: 19

6.2 The necessity for Fade duration: 19

6.3 Fade slope prediction model (ITU-R Model): 19

7 Results **21**

8 Conclusions **26**

BIBLIOGRAPHY

List of Figures

2.1 Two Layer Precipitation Model 5
2.2 k_H increases as frequency increases from 1 to 100 GHz 10
2.3 α_H increases as frequency increases upto 4 GHz and then it starts decreasing 10
2.4 k_v increases as frequency increases from 1 to 100 GHz 11
2.5 α_v increases as frequency increase from 1 to 6 GHz, and it starts decreasing after around 6 GHz 11

4.1 Experimental Setup 13

5.1 Horizontally polarized 20.2 GHz frequency signal on 21/7/2015 14
5.2 Rain event on 21/7/2015 14
5.3 Rain attenuation on 21/7/2015 15
5.4 Rain attenuation on 21/7/2015 15
5.5 Horizontally polarized 20.2 GHz frequency signal on 18/8/2015 16
5.6 Rain event on 18/8/2015 16
5.7 Rain attenuation on 18/8/2015 16
5.8 Rain attenuation on 18/8/2015 17

6.1 Fade Dynamics 18

7.1 Rain rate time series on 25/7/2015 21
7.2 Predicted attenuation time series by SST for rain event on 25/7/2015 . . 22
7.3 Rain rate time series on 22/7/2015 22
7.4 Predicted attenuation time series by SST for rain event on 22/7/2015 . . 22
7.5 Comparison between actual and predicted attenuation for rain event on 25/7/2015 23
7.6 Comparison between actual and predicted attenuation for rain event on 22/7/2015 23
7.7 Comparison between actual and predicted attenuation for all events. . . . 24
7.8 Comparison between actual and predicted Fade duration for all rain events 24
7.9 Comparison between actual and predicted Fade slope for all rain events . 25
7.10 Fade slope from ITU-R Model 25

List of Tables

2.1 k and alpha values for 20.2 GHz frequency 6
2.2 k and α values for horizontal and vertical polarization at different frequencies 9

Chapter 1

Introduction

At higher frequencies, the performances of satellite communication links are heavily affected due to the signal being subjected to numerous propagation obstacles such as rain attenuation, tropospheric scintillation, cloud, gaseous attenuation, etc. Fluctuations in the refractive index produce tropospheric scintillation in the initial few kilometers of altitude and are caused by temperature inversion layers and high humidity gradients. Gases present in the signal path also causes a reduction in signal level. The interaction between the gaseous constituents and the signal results in molecular absorption that causes a decrease in signal amplitude. Cloud and fog attenuation also affects radio wave propagation. They consist of water droplets with a diameter less than 0.1 mm, whereas the diameter of raindrops varies from 0.1 mm to 10 mm. For frequencies lower than 100 GHz, the fog attenuation is very low. Among all the impairments, rain attenuation is the most crucial in the propagation of high-frequency electromagnetic waves, resulting in immense variations in the collected power of the signal and less predictability. Given below are the various propagation mechanisms that can affect the characteristics of the signal.

1. **Absorption**: It reduces the signal amplitude, and the lost energy increases the internal energy of the molecule.

2. **Refraction**: It changes the direction of propagation of the signal due to the variations in the refractive index of the medium.

3. **Diffraction**: Due to the presence of an obstacle in the medium, there is a change in the direction of propagation of the signal.

4. **Multipath**: It results from irregularities in the refractive index of the medium, and the transmitted signal is received by the antenna by two or more propagation paths.

5. **Scintillation**: Rapid variations in the amplitude and phase of the signal due to the small-scale irregularities in the path with time.

6. **Fading**: Variations in the signal amplitude due to the changes in the signal path. Fading refers to slower variations with time, whereas scintillation includes rapid variation.

7. **Scattering**: The energy of the signal is dispersed in direction due to the inhomogeneities in the medium.

Raindrops cause:

1. Absorption and scattering of signals that result in rain attenuation.

2. Moreover, raindrops have non-spherical shapes that result in a change of polarization features of the transmitted signal, known as rain depolarization (i.e., energy transfer from one polarization state to another state).

Rain depolarization causes additional attenuation. Rain effects depends on drop shape, size distribution of raindrops, rainfall rate and to a lesser degree, on ambient temperature and pressure. Equatorial and tropical regions are the regions of heavy rainfall, and hence attenuation due to rain is a grave concern in such regions for high frequency links. It is amongst the primary obstacles to the effective operation of satellite communication links. Knowledge of rain fade characteristics are essential for applying the fade mitigation technique for the efficient operation of the communication link. The absence of actual data, particularly at higher frequencies, requires estimation of attenuation from rain rate time series, especially for tropical areas where the issue is severe.

The synthetic storm technique (SST) can produce time-sequential rain attenuation from rain data for any polarization and frequency. Rain rate time series is converted to rain rate space series along the satellite link path by using storm translation speed across the way, hence the name 'synthetic storm.' The SST technique has shown great potential for generation of rain attenuation time series and tested successfully for mid-latitude temperate regions. However, the performance of the same has not yet been fully explored over tropical regions. Given the change in rain characteristics over tropical and equatorial regions over the temperate regions, it is thus imperative to study the performance of the SST model over India.

For experimental measurements, the setup includes a rain gauge and disdrometer.The tipping bucket rain gauge measures the time instant of tipping when the bucket's predefined amount of water gets collected. We have used experimentally measured data of earth space link in Ahmedabad at 20.2 GHz frequency from Satellite GSAT-14 to analyze the validity of the synthetic storm technique. GSAT-14 is a geostationary satellite, and it was created to provide platform for new experiments. 17 rain events, as well as corresponding rain data, has been used for this purpose. Attenuation from the measured data is obtained by doing signal processing of the raw data, i.e., horizontally polarized 20.2 GHz of frequency. This attenuation is then compared with attenuation predicted by the synthetic storm model from the rain data. Similarly, the fade duration is calculated from actual data and compared with the SST model. And at last, the fade slopes from the actual data are compared with the fade slopes predicted by the SST model. Fade slopes are also compared with the ITU-R fade slope prediction model, a widely accepted model.

This work focuses on the performance evaluation of the synthetic storm model to convert experimentally obtained data of rainfall rate into attenuation due to rain.

The upcoming sections are as follows:

1. The synthetic storm technique.
2. Two-layer precipitation model.
3. Earlier work and other prediction models
4. Experimental setup.
5. Rain attenuation from measured data
6. Rain Fade dynamics.
7. Results and its analysis
8. conclusions.

Chapter 2

The Synthetic Storm Technique

2.1 Fundamentals of the Synthetic Storm Technique

The synthetic storm technique is helpful to improve the performance of satellite communication links and design satellite communication systems. Actual data for attenuation due to rain is not obtainable every time and is available only for a less number of sites and frequencies, but rain rate data is available globally. Under some assumptions, using the synthetic storm technique, attenuation due to rain can be obtained from converting instantaneous rainfall rate. The synthetic storm technique can predict a temporal series of attenuation due to rain for any inclined path above roughly 10° for any frequency and polarization.
The root of the synthetic storm technique is turning the time-sequential rainfall rate to a space series of rainfall rate across the line. This is done by convolution mathematically. Recorded rain rate changes with time due to the following two reasons:

1. Variations that happens within the time needed to pass over the rain gauge.

2. Advection.

Above two variations occur as rain pattern pass over the rain gauge.The rain gauge keep a record of these two effects along with the actual data, and it isn't easy to separate them.Tipping bucket rain gauge records the time series of rain rate. Transforming this series into a space series of rain rates can be made possible using a synthetic storm approach. This is done by estimation of storm translation velocity to convert time to distance. However, it doesn't provide accurate information on the spatial spread of rain as it only assumes advection. It is seen that rain rate statistics for many synthetic storms are almost comparable to those obtained from actual storms.
Application of the synthetic storm technique requires an understanding of the signal path length across the rain cell, velocity of rain cell, and rainfall rate at the site. The two-layer precipitation model and mathematical modelling are discussed in the following sections. Also, for this conversion, some assumptions are made that are also discussed.

2.2 Two layer Precipitation model

The troposphere is the lowest layer of the earth's atmosphere. Its vertical structure during rain can be divided into two layers as shown in Figure 2.1.

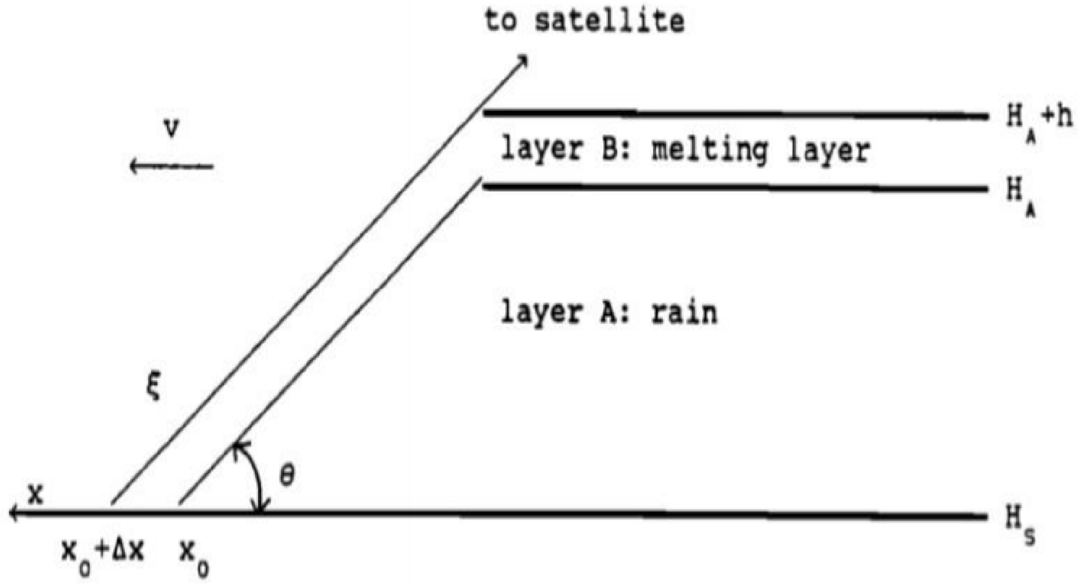

Figure 2.1: Two Layer Precipitation Model

1. Layer A or Rain layer with raindrops
2. Layer B or Melting layer with melting hydrometeors

Here, rainfall at different heights are modelled into a two-layer precipitation model. Starting from the surface, initially, there is a rain layer which is layer A that contains hydrometeors in the shape of raindrops accompanied by a melting Layer B (above layer A). This melting layer contains ice hydrometeors that turn into raindrops at the top of the rain layer. Assumption of constant vertical rainfall rate R (mm/hr) is made for layer A. Following are the assumptions that are made for calculating rain attenuation using synthetic storm technique as well to describe and specify layer B:

1. During melting, the mass of a hydrometeor (spherical) is constant (0.3g/cm is the assumed density of the unmelted core)
2. Between raindrops in rain layer and hydrometeors in layer B, there is a one-to-one correspondence.
3. Both the layers have the same flux of hydrometeors.
4. For layer B, specific attenuation is obtained as if it was received with a similar volume of melting hydrometeor by raindrops.
5. 400 m (0.4 km) is the height that is assumed for layer B (melting layer). It doesn't depend on the latitude of the site.

2.3 SST Model

Under these assumptions, it can be shown from the calculation that the vertical rainfall rate in layer B, named as apparent rainfall rate, can also be assumed to be constant and is as follows:

$$\boxed{R_B = 3.134 R_A}$$

$$\boxed{or \mathrm{R}_B = r.R_A}$$

'r' relates the rainfall rate of layer A with layer B

At any point (say x), the specific attenuation is given by:

$$\boxed{\gamma = k R^{\alpha}(x)}$$

where alpha and k are the essential parameters to link the specific attenuation with the rainfall rate. 20°c is the assumed temperature of raindrops of layer A whereas 0°c temperature for layer B, which contains melting hydrometeors. The constants k and alpha are given by ITU-R for Parson's law distribution of drop size and 20° c of water temperature. [From 1981 paper by Maggiori][6], the value of these parameters at 0°c is known. These two parameters at frequency 20.2 GHz are calculated for rain layer and melting layer and are shown in the table below:

Temperature (°c)	Frequency (GHz)	Layer	k	α
20	20.2	Layer A	0.09164	1.0568
0	20.2	Layer B	0.09611	0.9847

Table 2.1: k and alpha values for 20.2 GHz frequency

Following are the features of constants k and α:

1. These two constants represent complex behavior of specific attenuation.
2. These parameters depend on signal polarization, frequency and dispersal of the size of the raindrop.
3. They don't change with space and time.
4. These constants also depend on temperature.

Advection velocity of rain cell is used to convert time series of rainfall rate into attenuation using the following equation:

$$\boxed{x = vt}$$

Along the path, considering both the layers, signal attenuation is obtained by converting specific attenuation using the following expression:

$$\boxed{A(x) = K_A \int_0^{L_A} R^{\alpha_A}(x + \Delta x, \xi)\, d\xi \ + K_B r^{\alpha_B} \int_{L_A}^{L_B} R^{\alpha_B}(x, \xi)\, d\xi} \tag{2.1}$$

where,

- L_A and L_B are the signal path lengths in rain layer and melting layer respectively
- $A(x)$ denotes attenuation at a particular point.
- Δx denotes deviation due to Layer B

Following are the inputs that are needed to implement the synthetic storm technique for the location under consideration: According to ITU-R[8], the height of two layers can be calculated as: $\boxed{H_A = H_B - h}$
where,

- H_A= Height of layer A or rain layer above sea level
- H_B= Height of layer B above sea level
- h=thickness of melting layer

For current location, $\boxed{\text{h=400 m (or 0.4 km)}}$

The altitude of the Space application center, Ahmedabad

$\boxed{\text{H}_s\text{= 53 m = 0.053 km}}$

θ is the link elevation angle and its value in our case is 63°

From ITU-R:

H_B = 5, for latitude < 23°

And, H_B = 5 - 0.075 (latitude - 23°), for latitude ≥ 23°

H_B is calculated from above equation and in our case H_B is 4.9985

Therefore, $\boxed{\text{H}_A \text{ = 4.9985 - 0.4 = 4.5985 km}}$

Hence, the signal path length for this case is: $\boxed{\mathrm{L}_A = (H_A - H_s/sin\theta) = 5.101 \text{ km}}$

And, $\boxed{\mathrm{L}_B = (H_B - H_S/sin\theta) = 5.550 \text{ km}}$

Therefore, $\boxed{(\mathrm{L}_B - L_A) = 0.4717 \text{ km}}$

The following equation was obtained by using the theory of Fourier transforms under some assumptions in Matricciani, 1996[1].

$$\boxed{A(t) = K_A R^{\alpha_A}(t) L_A + r^{\alpha_B} K_B R^{\alpha_B}(t)(L_B - L_A)} \tag{2.2}$$

where

R(t)= Time series of rainfall rate

A(t)= Attenuation time series

The equation 2.2 is the key equation that is used for obtaining rain attenuation time series from rain rate time series.

2.4 Variation of k and α with frequency (GHz)

International Telecommunication Union (ITU) has provided the values of coefficients k and α for horizontal and vertical polarization at different frequencies[7]. The table is given below:

Frequency in GHz	k_H	k_v	α_H	α_v
1	0.0000259	0.0000308	0.9691	0.8592
2	0.0000847	0.0000998	1.0664	0.9490
4	0.0001071	0.0002461	1.6009	1.2476
6	0.007056	0.0004878	1.5900	1.5882
7	0.001915	0.001425	1.4810	1.4745
8	0.004115	0.003450	1.3905	1.3797
10	0.01217	0.01129	1.2571	1.2156
12	0.02386	0.02455	1.1825	1.1216
15	0.04481	0.05008	1.1233	1.0440
20	0.09164	0.09611	1.0586	0.9847
25	0.1571	0.1533	0.9991	0.9491
30	0.2403	0.2291	0.9485	0.9129
35	0.3374	0.3224	0.9047	0.8761
40	0.4431	0.4274	0.8673	0.8421
45	0.5521	0.5375	0.8355	0.8123
50	0.6600	0.6472	0.8084	0.7871
60	0.8606	0.8515	0.7656	0.7486
70	1.0315	1.0253	0.7345	0.7215
80	1.1704	1.1668	0.7115	0.7021
90	1.2807	1.2795	0.6944	0.6876
100	1.3671	1.3680	0.6815	0.6765

Table 2.2: k and α values for horizontal and vertical polarization at different frequencies

It is observed that:

1. k_H increases as frequency increases from 1 to 100 GHz.
2. α_H increases as frequency increases upto 4 GHz and then it starts decreasing.
3. k_v increases as frequency increases from 1 to 100 GHz.
4. α_v increases as frequency increase from 1 to 6 GHz, and it starts decreasing after around 6 GHz.

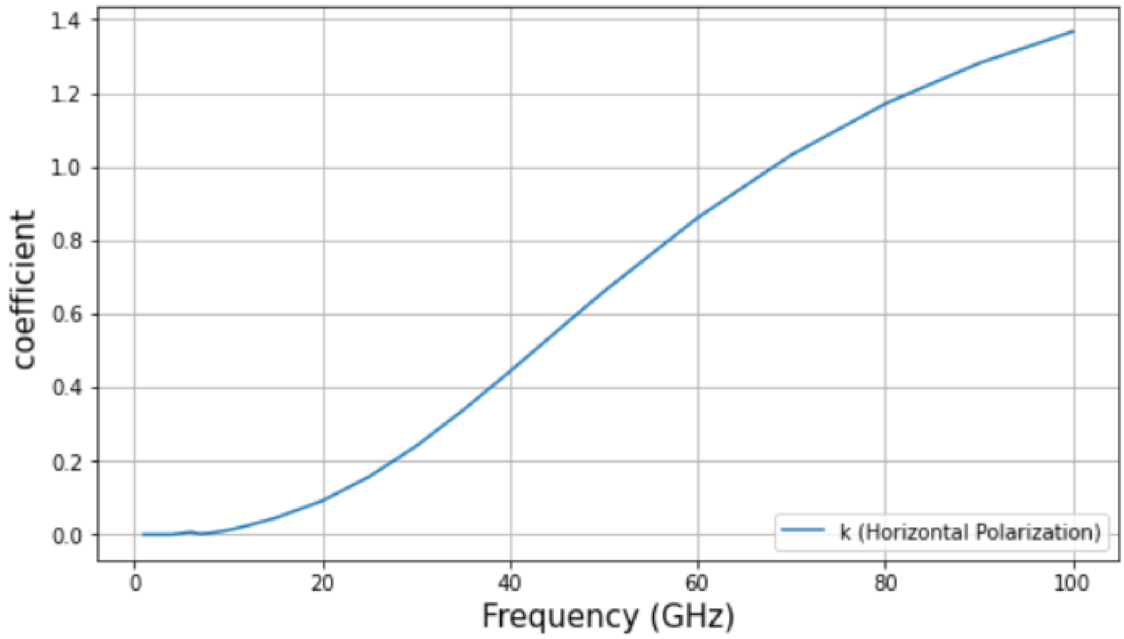

Figure 2.2: k_H increases as frequency increases from 1 to 100 GHz

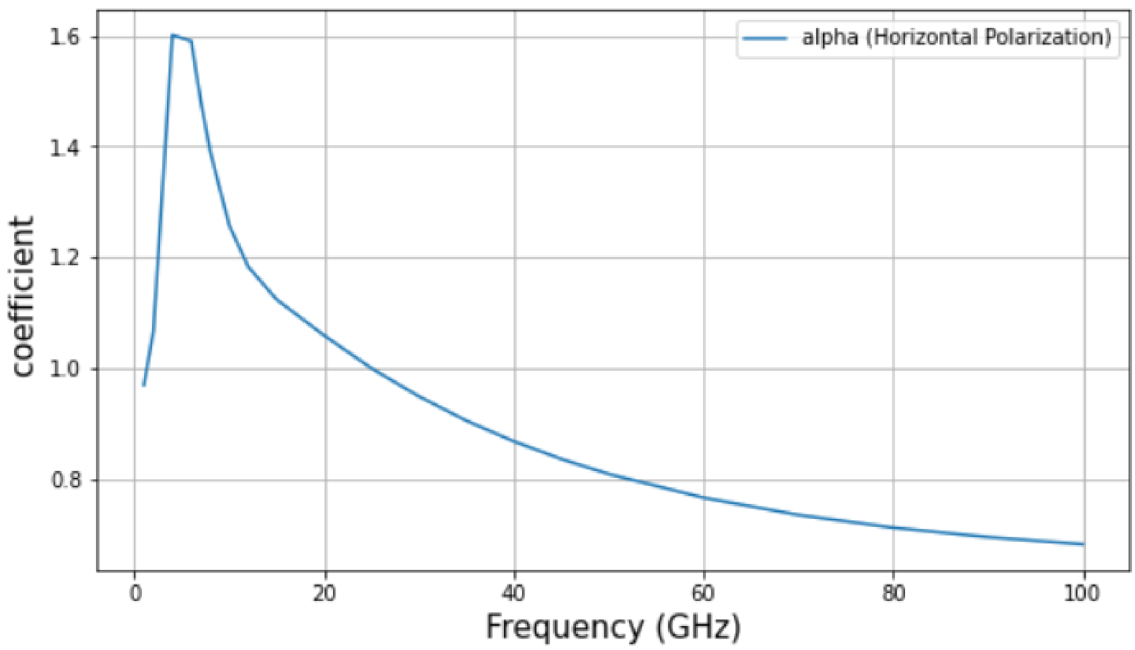

Figure 2.3: α_H increases as frequency increases upto 4 GHz and then it starts decreasing

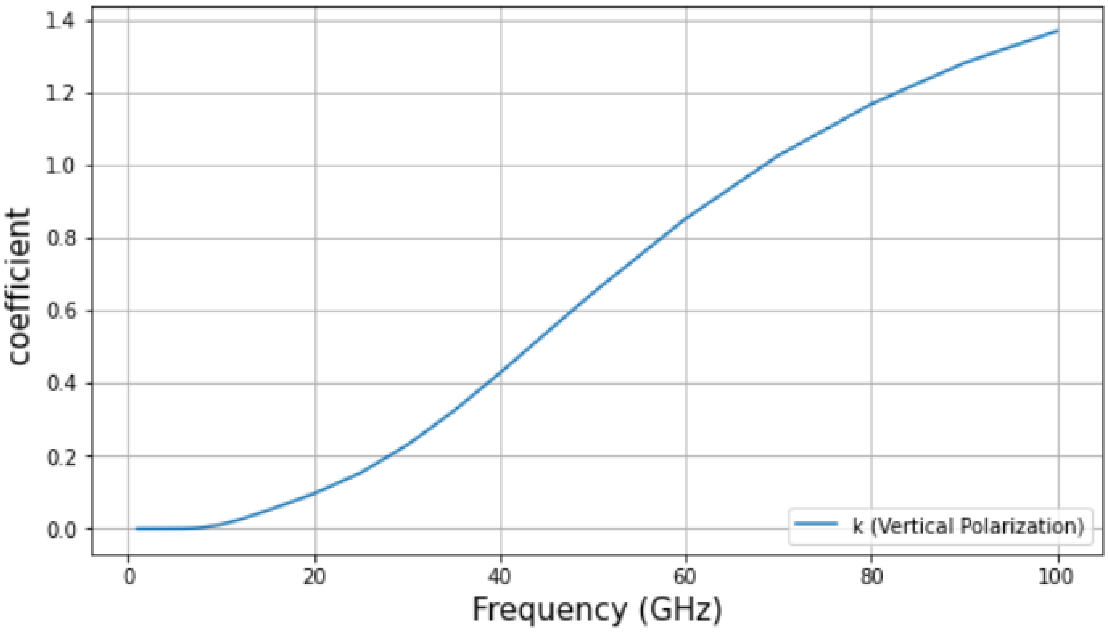

Figure 2.4: k_v increases as frequency increases from 1 to 100 GHz

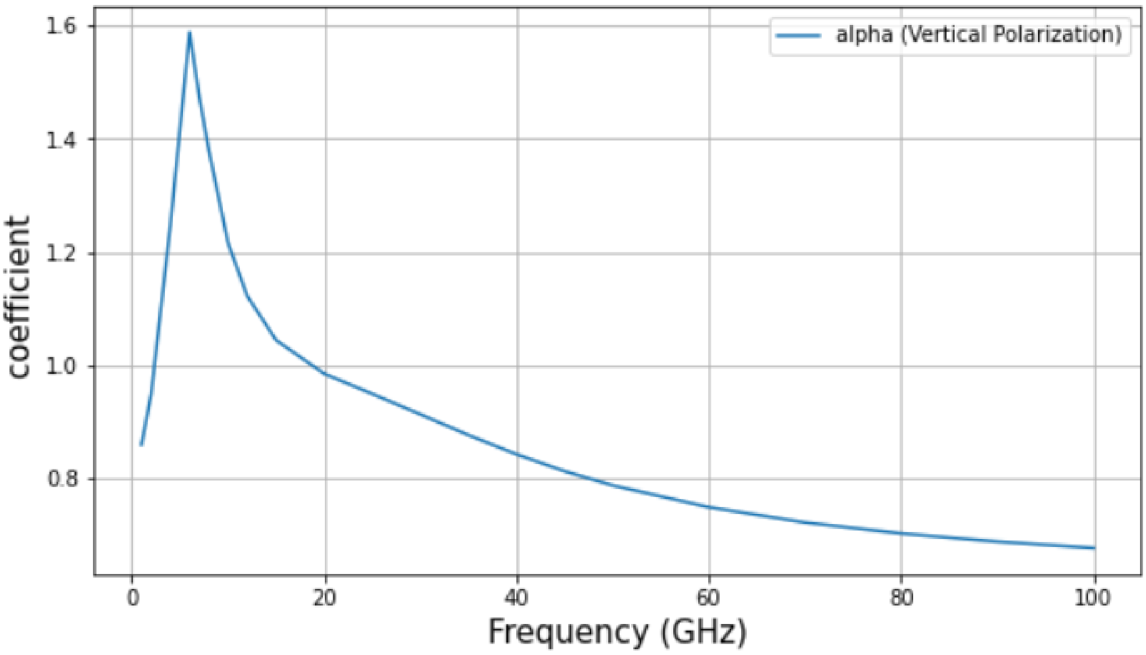

Figure 2.5: α_v increases as frequency increase from 1 to 6 GHz, and it starts decreasing after around 6 GHz

Chapter 3

Earlier work and other prediction models:

Various efforts have been made to predict and model long-term statistics of rain attenuation to help design communication links. However, actual data is undoubtedly restricted to particular sites and parameters of the link. Due to this reason, various models are often applied to estimate rain attenuation., For example, the ITU-R model, Crane Global Model, etc. Various models have different input parameters as well as specific estimation tools. Classification of multiple models is given below:

1. **Empirical Model:** Such a model doesn't use mathematically defined input-output relations and makes use of experimental data.
2. **Physical model:** It uses relations between the physical structure of rain events and rain attenuation model's formulation.
3. **Statistical model:** It makes use of data analysis, and lastly, the model is produced as a result of regression analysis in often cases.
4. **Fade slope model:** Attenuation slope versus time data is utilized to estimate attenuation due to rain.

The synthetic storm is a physical-mathematical model that predicts attenuation time series from rainfall rate time series. Recently, it has been an effective and precise tool that can generate all the required statistics of attenuation due to rain and surmounts the other models.

The synthetic storm technique has been analyzed at:

1. Q-band and Ka-band in Vigo, Spain, at a temperate location[5],
2. Malaysia at 10 GHz frequency[2]. etc.,

However, the model's performance has not yet been fully explored over tropical regions for particular bands. Given the change in rain characteristics over tropical and equatorial areas over the temperate regions, it is thus essential to study the effectiveness of the SST model over India for different locations on numerous frequency bands.

Chapter 4

Experimental Data

From Ist July 2015 to 31st August 2015, the horizontally polarized K-band satellite signal from GSAT-14 has been continuously monitored (23.02° N, 72.51° E) at the Space Application Centre (SAC) Ahmedabad. At K-band, 20.2 GHz of signal has been collected by an antenna. The earth-satellite elevation angle is 63°. There is a tipping bucket rain gauge that is used to measure rainfall rate, which records rainfall rate after every 60 seconds of time interval and hence the rain events, as shown in the figure below:

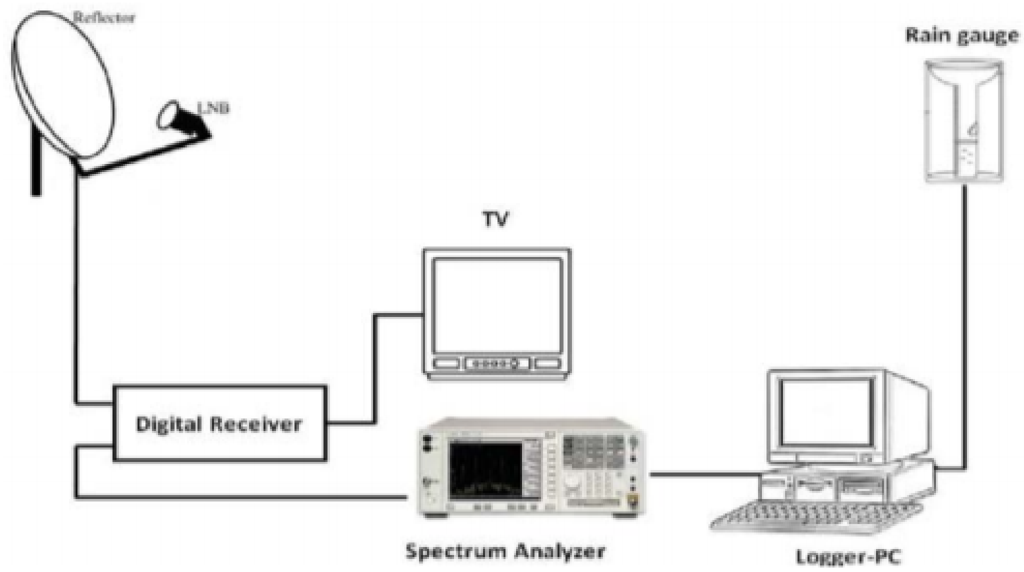

Figure 4.1: Experimental Setup

Chapter 5

Rain attenuation from measured data

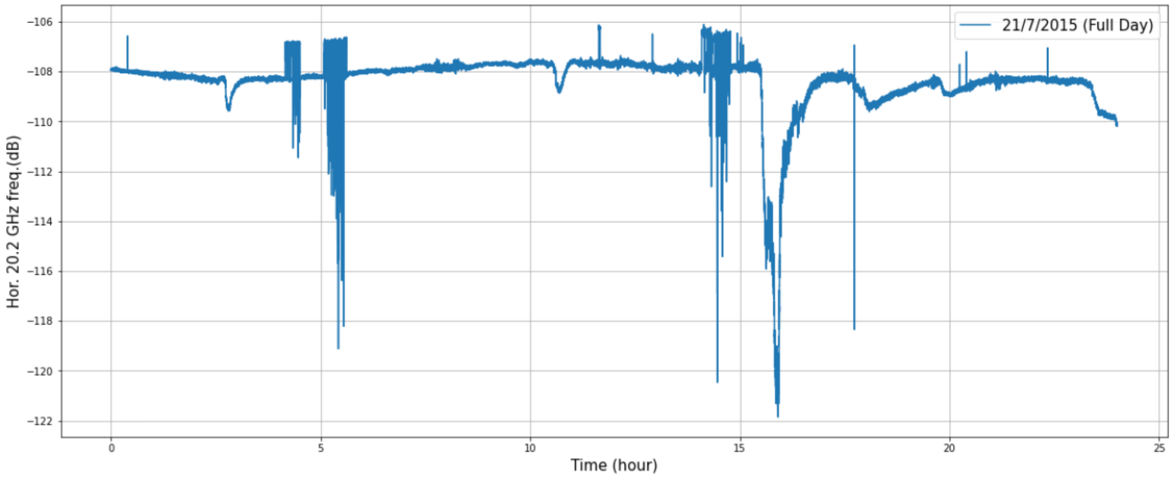

Figure 5.1: Horizontally polarized 20.2 GHz frequency signal on 21/7/2015

Above plot shows the horizontally polarized 20.2 GHz frequency on 21/7/2015. The rain event is extracted from the above graph where the rain attenuation has occurred.

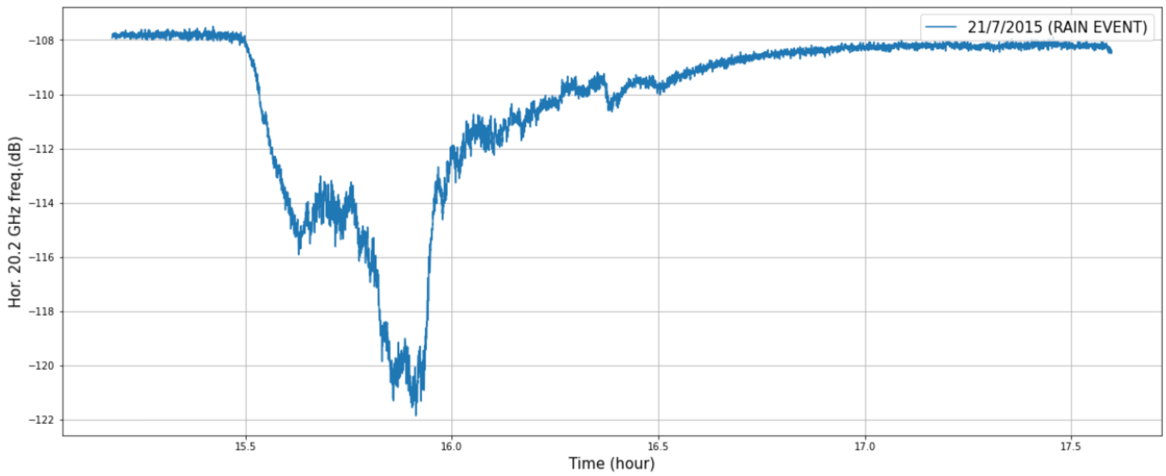

Figure 5.2: Rain event on 21/7/2015

Figure 5.2 shows the rain event extracted from the signal on 21/7/2015 in figure 5.1. To obtain the positive values of attenuation, each value of the rain event in figure 5.2 is subtracted from the average of the endpoints of the same rain event. After doing so, the following graph is obtained.

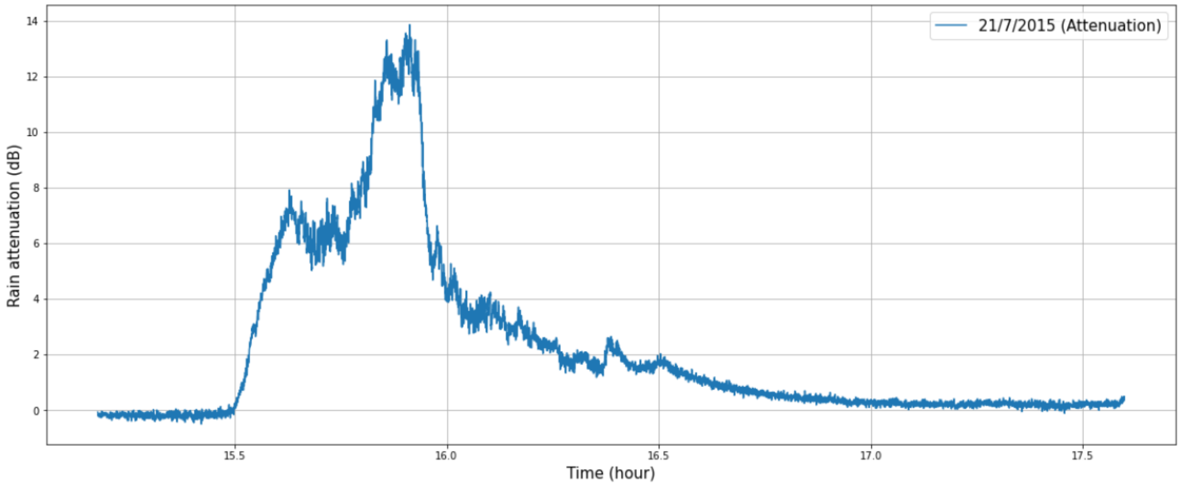

Figure 5.3: Rain attenuation on 21/7/2015

There are rapid fluctuations in figure 5.3 that can be seen. Therefore, a Butterworth low pass filter of 10th order and cutoff frequency 0.025 Hz is used to remove the rapid fluctuations and scintillations.

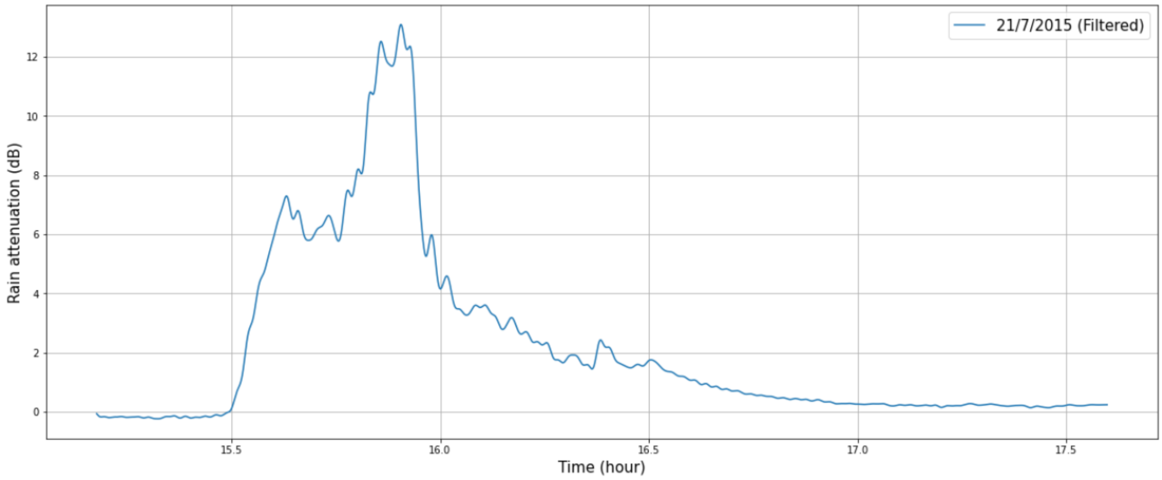

Figure 5.4: Rain attenuation on 21/7/2015

After signal processing shown above, rain attenuation in figure 5.4 is the final attenuation used for the analysis as rain attenuation from the measured data.

Similarly, the signal processing for another rain event on 18/8/2015 is shown in figure 5.5, 5.6, 5.7, 5.8

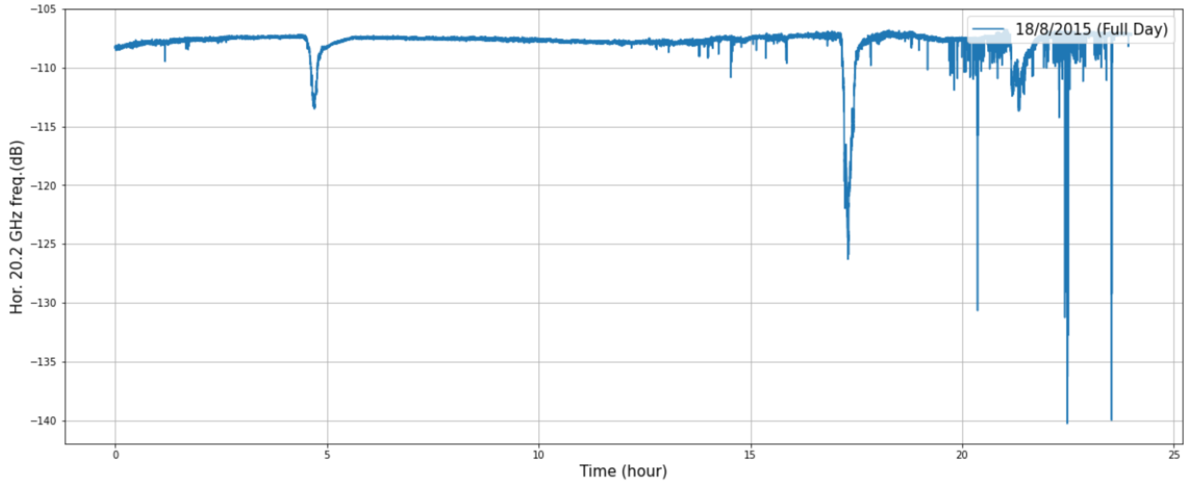

Figure 5.5: Horizontally polarized 20.2 GHz frequency signal on 18/8/2015

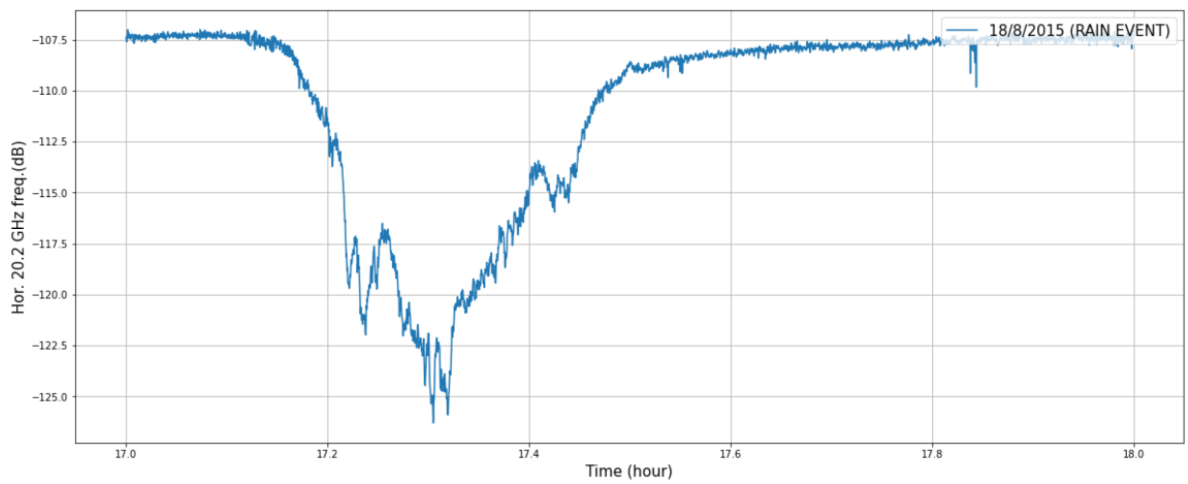

Figure 5.6: Rain event on 18/8/2015

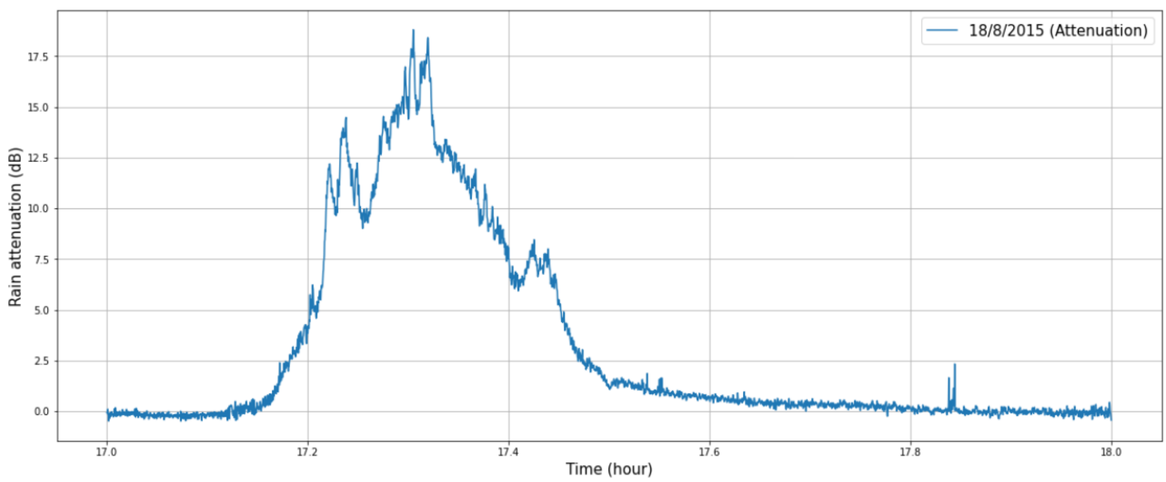

Figure 5.7: Rain attenuation on 18/8/2015

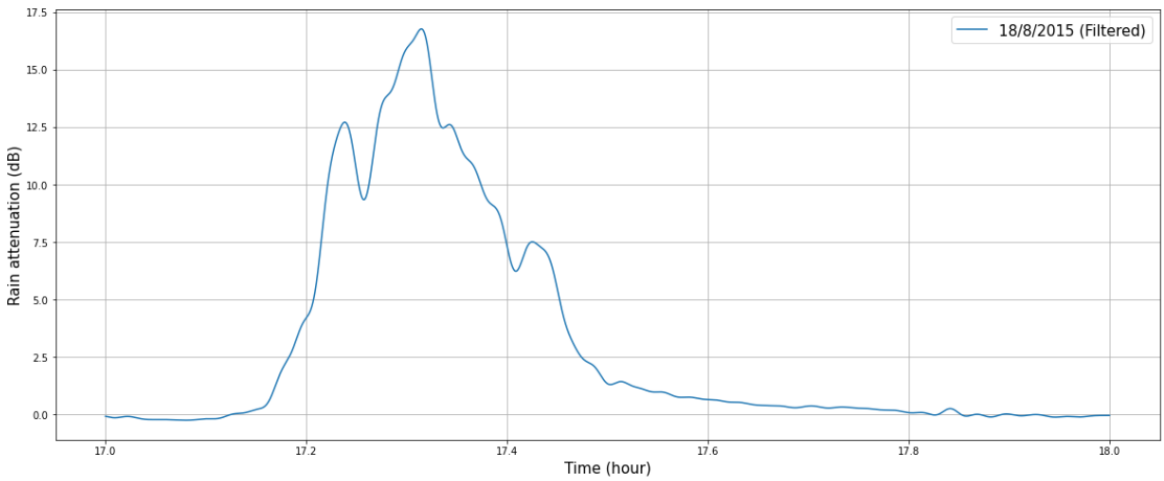

Figure 5.8: Rain attenuation on 18/8/2015

This signal processing is done for all 17 events to obtain rain attenuation from the measured data.

Chapter 6

Rain Attenuation Dynamics

Rain attenuation dynamics are helpful for the application of Fade mitigation techniques for designing communication links. For a given attenuation, rain attenuation dynamics include the following three characteristics:

1. Fade slope
2. Fade duration
3. Interfade duration

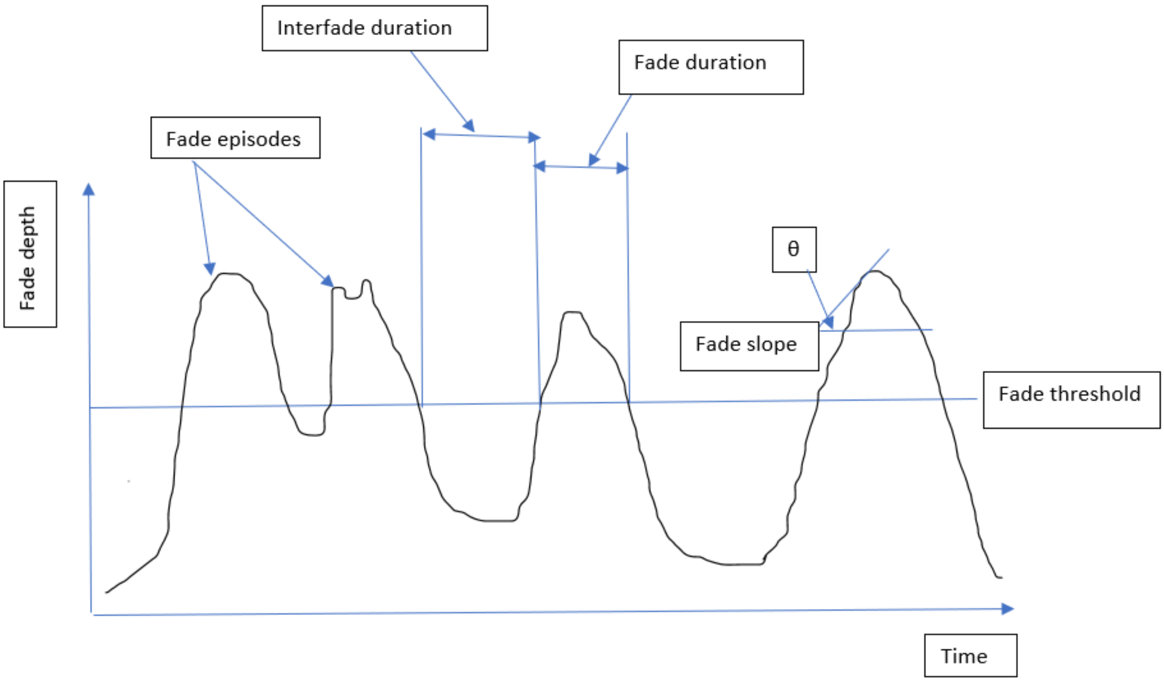

Figure 6.1: Fade Dynamics

These three characteristics are helpful to maintain the performance and dependability of the system.

- The rate of change of fade with time is called **fade slope**.
- The period of rain fade above a particular threshold of attenuation is called **fade duration**.
- **Interfade duration** is the period of rain fade below the fade threshold. It is crucial to know this duration statistically before another outage event.

6.1 The necessity for Fade slope:

- The fade slope is the rate of change of fade with time. The information of the fade slope of the collected signal helps design a control loop that can trace variations in signals.
- The slope of the gradually changing part of the signal is the crucial information that includes filtering out rapid fluctuations and scintillations.

6.2 The necessity for Fade duration:

The period of rain fade above a particular threshold of attenuation is called fade duration. It is an essential parameter in system designing for numerous reasons. Given below are the various reasons that make fade duration information vital:

1. Information of fade duration provides the number and period of outages and unavailability of the system.
2. It is essential to understand the event duration to assign the resource to other users.
3. Attenuation duration is a crucial component in the process of selecting forward error correction code and choosing the best modulation schemes.

6.3 Fade slope prediction model (ITU-R Model):

In 2003, the International telecommunication union (ITU) came up with the ITU-R model to calculate fade slope characteristics due to rain attenuation in communication links[9]. The probability distribution of fade slope was found to rely on the size distribution of drop and climate parameters. Moreover, it depends on rain attenuation, rain type and time interval. It also has a dependence on the cut-off frequency of the low pass filter to filtrate rapid fluctuations and scintillations. It is essential to remove rapid fluctuations and scintillation of attenuation due to rain. Otherwise, the signal shows high fluctuations, resulting in poor matching as the model will only predict the attenuation due to rain. Experimentally, efficient filtering of rapid fluctuations and scintillations has been found using a low pass filter having cut-off frequency of 0.025 Hz. Model is applicable for the below-given parameters:

1. 10-30 GHz frequency range.

2. 10 - 50 degrees of elevation angles.

Below given are the parameters that are needed as input data in the model:

- 0 to 20 dB: Attenuation level
- 0.001 to 1 Hz: f_B
- 2 to 200s: Length of time interval

Following are the steps used for fade slope while calculating its probability distribution using the ITU-R standard model:

1. Calculate the function having dependence on f_B and time period over which fade slope is computed.

$$F(f_B, \Delta t) = \sqrt{2\pi^2/((1/f_B^b) + (2\Delta t)^b)^{1/b}}.$$

   where,
   b=2.3

2. At given attenuation, calculate the standard deviation using below equation.

$$\sigma_\xi = sF(f_B, \Delta t)A$$

   where,
   Parameter s depends on climate and elevation angle, and its value is 0.011

3. At given attenuation, calculate the conditional probability of fade slope

$$P(\xi/A) = 2/(\pi\sigma_\xi(1 + (\xi/\sigma_\xi)^2)^2$$

   where,
   $P(\xi/A)$ is conditional probability density

Chapter 7

Results

A total of 17 rain events have been used for the analysis. Using the SST model, from equation 2.2, these events are converted into time series of rain attenuation. Values of k and α for horizontally polarized 20.2 GHz frequency at two different temperatures are given in the table 2.1.

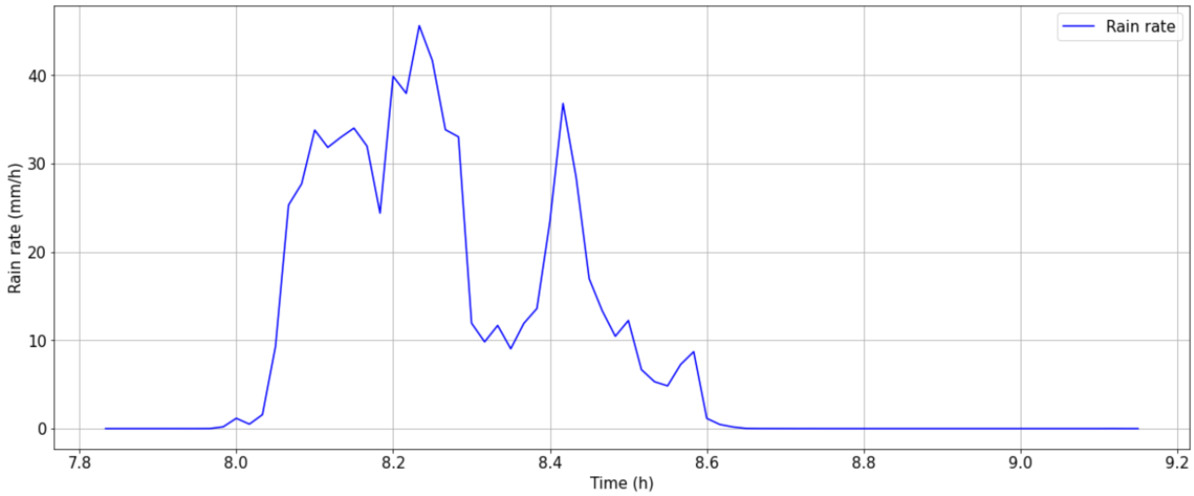

Figure 7.1: Rain rate time series on 25/7/2015

Figures 7.1 and 7.3 are the two rain rate time series, whereas figure 7.2 and 7.4 are their corresponding attenuation series. Following are the observations from these figures:

1. The predicted time series of attenuation is observed to follow the same pattern as the rain rate time series.
2. A high correlation between the time series of rainfall rate and attenuation predicted by the synthetic storm technique.

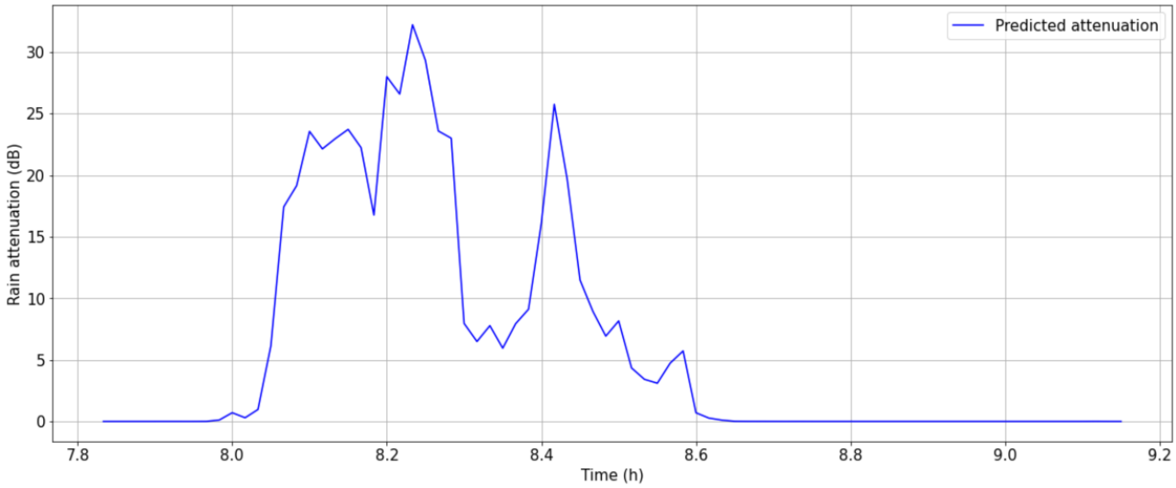

Figure 7.2: Predicted attenuation time series by SST for rain event on 25/7/2015

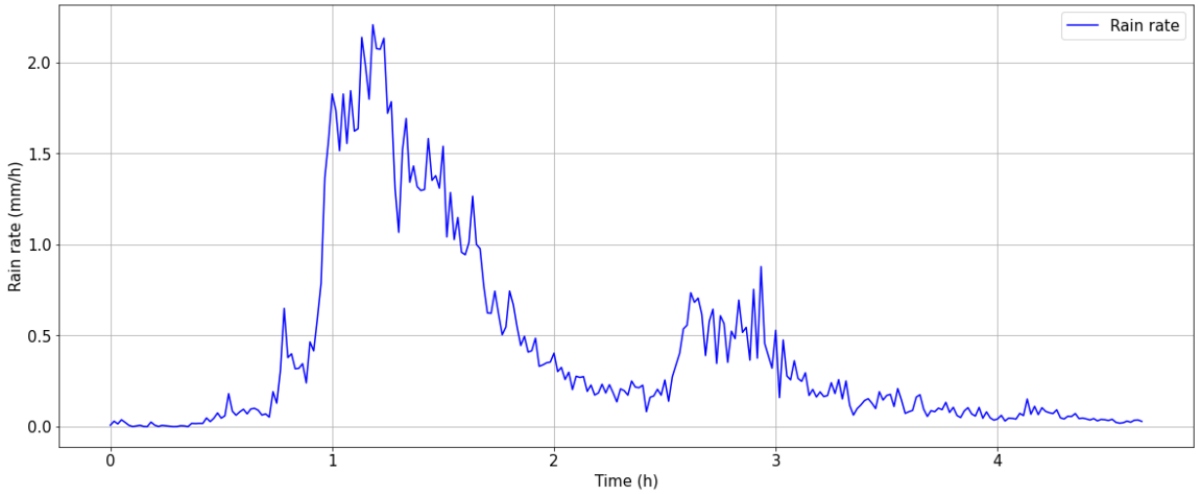

Figure 7.3: Rain rate time series on 22/7/2015

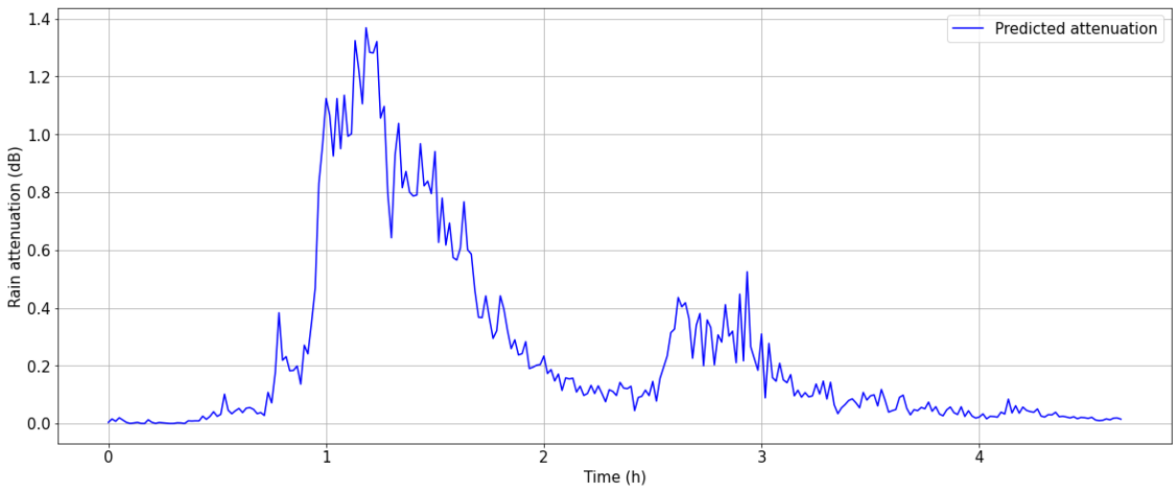

Figure 7.4: Predicted attenuation time series by SST for rain event on 22/7/2015

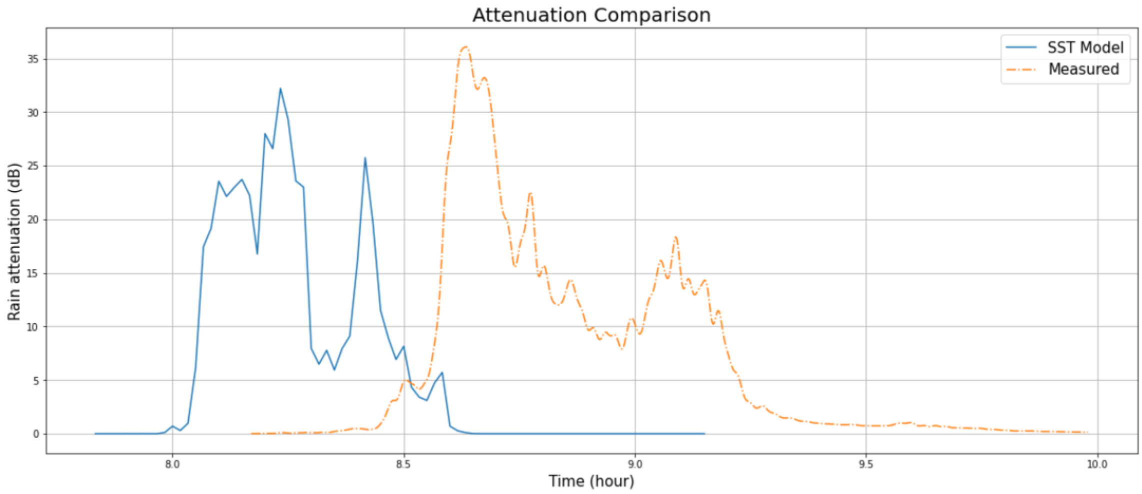

Figure 7.5: Comparison between actual and predicted attenuation for rain event on 25/7/2015

In figures 7.5 and 7.6, there is a comparison between the actual and predicted attenuation for rain events on 25/7/2015 and 22/7/2015, respectively. Following are the observations from the figures:

1. There are various peaks in Figures 7.5 and 7.6. In figure 7.5, the maximum peak of rain attenuation is approximately 37 dB, whereas it is around 32 dB from SST Model.
2. There is a time mismatch in figures 7.5 and 7.6. This mismatch may happen due to the resynchronization of measurement devices. It is significant in figure 7.5.

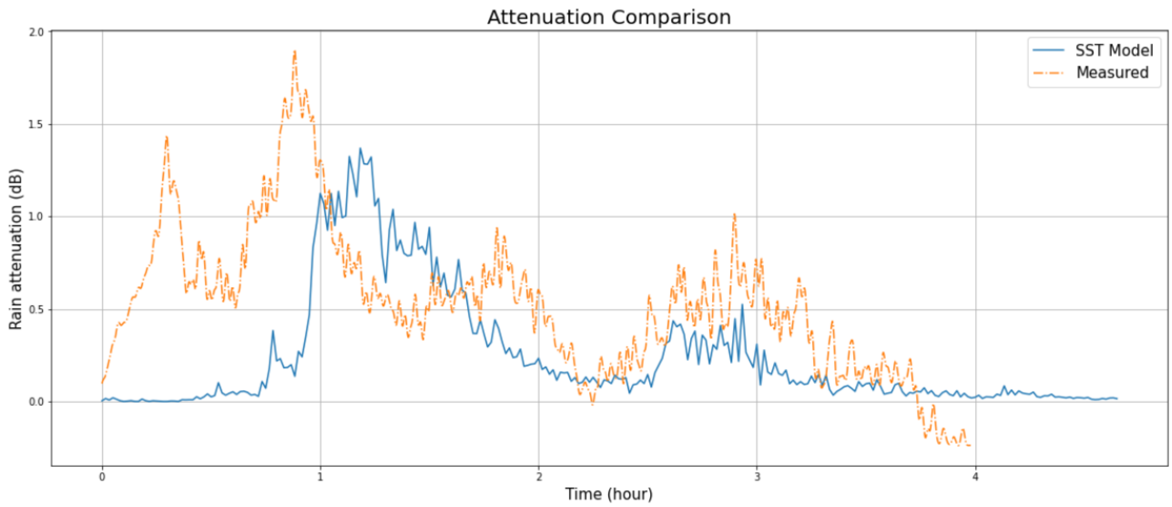

Figure 7.6: Comparison between actual and predicted attenuation for rain event on 22/7/2015

Similarly, in figure 7.6, the maximum peak of rain attenuation is about 2 dB, whereas it is approximately 1.4 dB from SST Model. However, some events have a massive difference in measured and predicted attenuation .

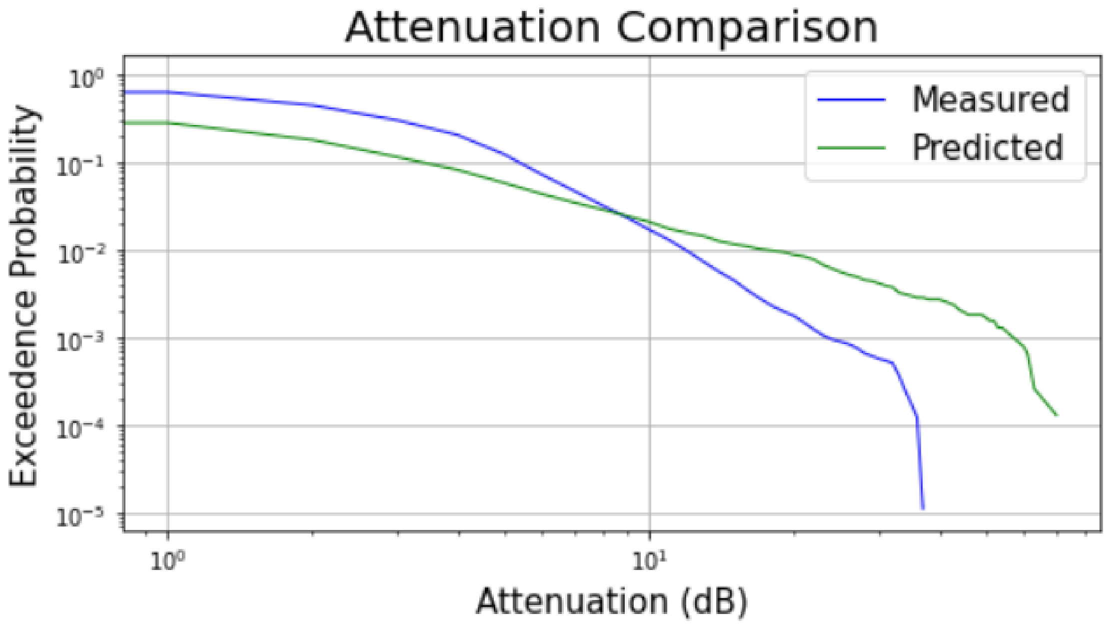

Figure 7.7: Comparison between actual and predicted attenuation for all events.

An attenuation comparison for all the 17 events is shown in figure 7.7. Again, it is seen that the predicted rain attenuation matches the measured rain attenuation at around 8 dB. However, before it, the synthetic storm technique is underestimated, and after it, it is overestimated.

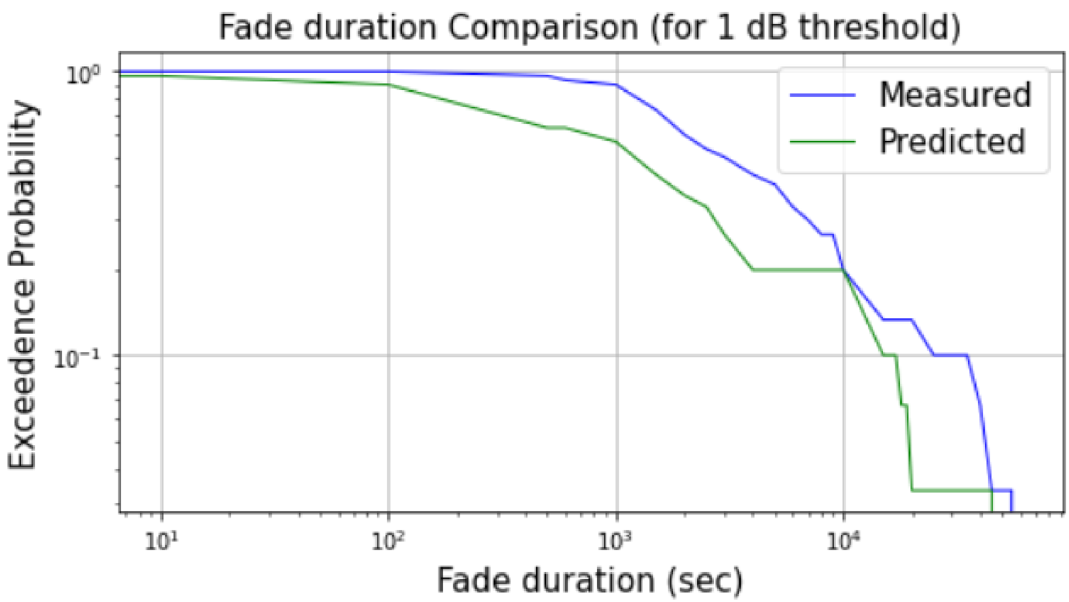

Figure 7.8: Comparison between actual and predicted Fade duration for all rain events

The fade duration comparison matches at some points, whereas fade duration is underestimated for the rest of the points.

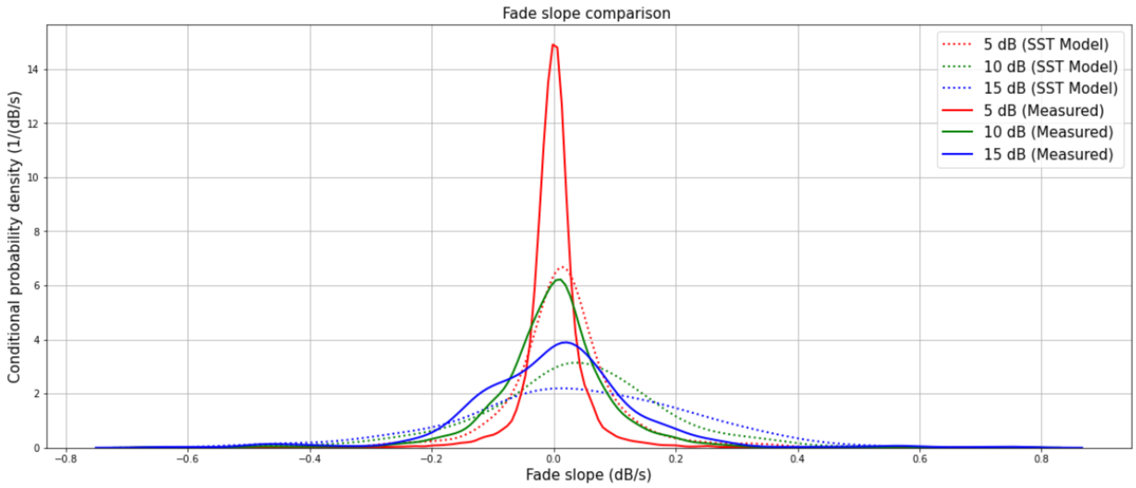

Figure 7.9: Comparison between actual and predicted Fade slope for all rain events

In figure 7.9, The conditional probability density of the predicted fade slope by SST is almost half of the fade slope from the measured data for the lower values. The mismatch decreases at higher values. Mismatch also decreases with the increasing attenuation threshold. This is also observed in figure 7.10 between the fade slopes predicted by SST and ITU-R fade slope prediction model. ITU-R fade slope prediction model almost matches with the fade slopes from actual data.

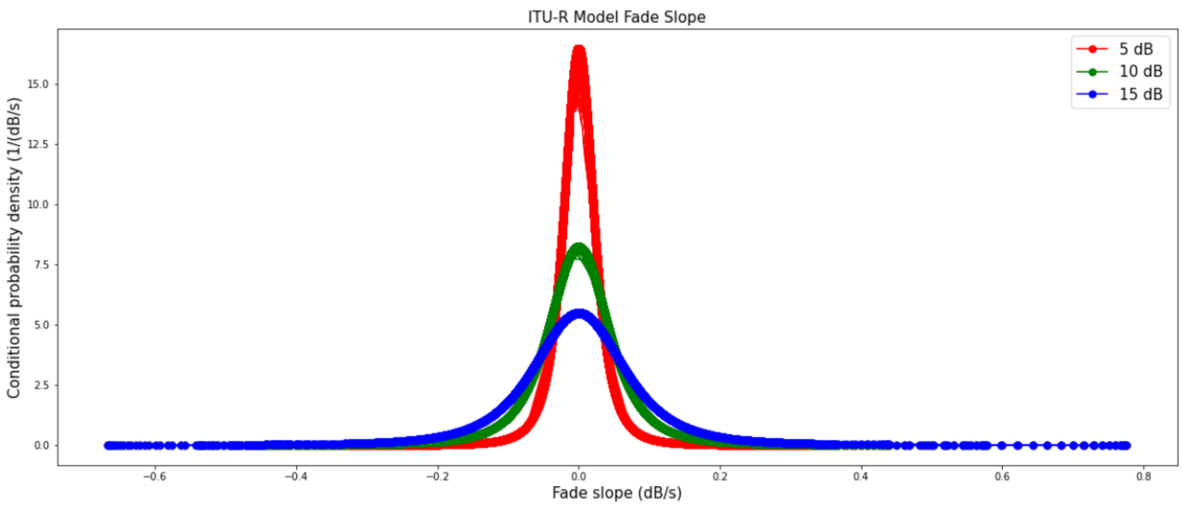

Figure 7.10: Fade slope from ITU-R Model

Chapter 8

Conclusions

This work is focused on testing the SST model for the prediction of rain attenuation at 20.2 GHz frequency. In this work, 17 events have been used for testing the model. Similarities between the model and actual data have been found. Along with this, there are underestimations and overestimations by the synthetic storm model. For the 17 events, in figure 7.8, the fade duration comparison matches at some points, whereas it is underestimated for the rest of the points. In figure 7.9, the conditional probability density of predicted fade slope by SST is almost half of the fade slope from the measured data for the lower values, whereas the mismatch decreases at higher values and also with the increasing attenuation threshold. The same is observed in figure 7.10 between the fade slopes predicted by SST and ITU-R fade slope prediction model. However, these results are preliminary, and the SST model strictly needs to be tested with more data having long-term measurements to validate the above results.

Bibliography

[1] Matricciani E 1996 Physical-mathematical model of the dynamics of rain attenuation based on rain rate time series and a two-layer vertical structure of precipitation: Radio Science Vol. 31 No. 2 pp. 281–295

[2] Rain Attenuation Analysis using Synthetic Storm technique in Malaysia A K Lwas, Md R Islam, J Chebil, M H Habaebi, A F Ismail, A Zyoud and H Dao Kulliyyah of Engineering International Islamic University Malaysia Jalan Gombak, 53100 Kuala Lumpur, Malaysia

[3] A Survey of Rain Attenuation Prediction Models for Terrestrial Links—Current Research Challenges and State-of-the-Art Md Abdus Samad, Feyisa Debo Diba and Dong-You Choi

[4] The Prediction of Rain Fade Slope on Satellite Link and calculation of the Slope of the Attenuation component from Measured Time Series, K.Kalyana Srinivas, Dr.T.Venkata Ramana, S.S.S.R.Rao, Y.Ravi Shekhar

[5] Application of synthetic storm technique for rain attenuation prediction at Ka and Q band for a temperate Location, Vigo, Spain Dalia (Das) Nandi, Fernando Pe´rezFonta´, Vicente Pastoriza-Santos b, Fernando Machado b an IIIT, Indian Institute of Information Technology Kalyani, West Bengal, India University of Vigo, Telecom Engineering School, Vigo, Spain

[6] Maggiori D, 1981 Computed transmission through rain in the 1–400 GHz frequency range for spherical and elliptical drops and any polarization Alta Frequenza, Vol. 50 pp. 262–273

[7] ITU-R P.838-3, 2005 Specific attenuation model for rain for use in prediction methods ITU-R Recommendations Geneva.

[8] ITU-R P.839-0: Rain height model for prediction methods. Recommendation P. Series Fascicle Radio wave propagation International Telecommunication Union Geneva

[9] ITU-R P.1623, Prediction method of fade dynamics on Earth-space paths